ELSEVIER

Ceramics International 28 (2002) 575–583

CERAMICS INTERNATIONAL

www.elsevier.com/locate/ceramint

# Characterization of Egyptian dolomitic magnesite deposits for the refractories industry

M.A. Serry[a,*], M.B. El-Kholi[a], M.S. Elmaghraby[a], R. Telle[b]

[a]*National Research Center 12622, Dokki, Cairo, Egypt*
[b]*Institute of Industrial Mineralogy, RWTH-Aachen, 52064 Aachen, Germany*

Received 14 September 2001; received in revised form 12 October 2001; accepted 26 November 2001

**Abstract**

Four technological samples representing pure and impure dolomitic magnesite deposits, recently explored in the Sul Hamed area, Eastern Desert, Egypt were investigated for their chemical and mineralogical composition. XRD, DTA, DTG, TG and wet chemical analysis methods were applied. Suitability of these deposits for manufacturing shaped and unshaped MgO–CaO refractories was assessed by studying their rate of densification on firing up to 1550 °C. The results were interpreted in the light of changes which occurred in phase composition and microstructure of the fired samples. Solid phase composition was qualitatively determined by XRD, where solid and liquid phases coexisting at 1300 and 1550 °C were calculated using the available phase equilibrium data. Microstructure and microchemistry of the dense samples were investigated by SEM and EDAX techniques. According to the research output, pure magnesites with the addition of MgO- and/or $Fe_2O_3$-rich materials are recommended for the production of unshaped MgO–CaO refractories. On the other hand, impure deposits can be utilized in manufacturing stable and semi-stable shaped MgO–dolomite refractories with and without addition of proper amounts of iron-rich material. 

*Keywords:* E. Refractories; Dolomite magnesite deposits; Characterization

## 1. Introduction

Shaped and unshaped basic refractories, based on magnesia and/or lime are produced world-wide for lining industrial furnaces, especially primary and secondary steel furnaces. For their production, dolomite and/or lime raw materials are fired in rotary or shaft kilns up to dead burning temperatures of 1500–1800 °C, using single- or double-stage firing processes. Accordingly, densification is accelerated in the solid state and/or by liquid phase leading to the production of volume-stable, dense and refractory MgO–CaO grains [1,2].

In the case of impure raw materials, densification mostly takes place by liquid phase without any addition using a single-stage firing at temperatures as low as 1500–1600 °C and the produced grains have low bulk density as well as suitable refractory quality. On the other hand, high refractory grains with maximum bulk density are obtained on dead burning of pure material using a double stage firing process. This includes calcination at 900–1200 °C, repowdering, reforming and refiring up to 1600–1800 °C. These grains are mostly sintered in the solid-state up to 1800 °C using a suitable dopant material to accelerate its sintering rate [3,4].

According to the technical reports issued in 1998 by the Egyptian Geological Survey, magnesite deposits existing in the Eastern Desert are unsuitable in some occurrences and promising in others [5]. The most promising occurrences explored in the Gabal Sul Hamed area occur as lenses, veins and/or pockets. Detailed field, mineralogy and geochemistry studies of these deposits were described elsewhere [6–8]. It is concluded that about 0.5 million tons of dolomitic magnesite rock with variable dolomite and calcite contents exist as hills, domes and veins in this area.

The aim of the present work is to assess the suitability of the dolomitic magnesite deposits of the Sul Hamed area existing South East of the Egyptian Eastern Desert for manufacturing shaped and unshaped MgO–CaO refractories. This includes chemical, mineralogical and

* Corresponding author. Tel.: +20-2-760-4124; fax: +20-2-337-0931.
*E-mail address:* mohamed_serry@hotmail.com (M.A. Serry).

0272-8842/02/$22.00 
PII: S0272-8842(02)00012-3

textural studies of these deposits before and after firing up to 1550 °C.

## 2. Experimental

Four technological samples were made from the different magnesite occurrences in the Sul Hamed area. Magnesite deposits existing as hills were classified into two categories and referred to as HP and HI, representing pure and impure types, respectively. On the other side, DP and DI also represent pure and impure magnesite samples collected from domes and veins. This classification is based on the degree of contamination of the white magnesite ore with the coloured serpentine and iron-oxide minerals. Fifty kilograms from each technological sample were prepared after manual classification into pure (HP and DP) as well as impure (HI and DI), which had low- and high-degrees of contamination with the coloured minerals.

The four technological samples (HP and HI as well as DP and DI) were crushed by a jaw crusher and finely ground in a steel ball mill to pass 100 μm sieve. Chemical and mineralogical composition of these representative samples were investigated using a proper scheme of wet silicate analysis as well as XRD, DTA, TG and DTG methods. XRD analysis was carried out using a Philips diffractometer PW/390, whereas a Perken-Elmer 7 series thermal analysis system was applied for thermal analysis, i.e. DTA, TG and DTG. Cylindrical samples of 25 mm diameter and about 25 mm height were semi-dry pressed under 50 $N/mm^2$ for each sample. The formed samples were then dried overnight at 110 °C and subsequently fired for 2 h between 1300 and 1550 °C with an interval of 50 °C. The fired samples were tested for their densification parameters as well as phase composition and microstructure. Solid-phase composition was qualitatively determined by XRD, while solid and liquid phases were quantitatively calculated at $<1300$, 1300 and 1550 °C using the available phase equilibrium data. Microstructure of some selected dense samples was investigated using a Philips SEM of model XL30 attached with an EDAX unit.

## 3. Results and discussion

Fig. 1 shows XRD patterns of the four technological samples: HP, HI, DP and DI. It is evident that HP is the most pure sample, it is mainly composed of magnesite mineral ($MgCO_3$), in addition to a small amount of dolomite [Ca, Mg $(CO_3)_2$]. The amount of dolomite increases in HI with the presence of appreciable amount of antigorite serpentine mineral [$Mg_3$ $Si_2$ $O_7$ $(OH)_2$]. On the other hand, DP and DI samples show some calcite mineral ($CaCO_3$) in addition to variable amounts of dolomite and serpentine minerals, beside the major magnesite mineral. The presence of dolomite and calcite minerals is confirmed by DTA, and DTG and TG analysis as shown in Figs. 2 and 3, respectively. Both DP and DI samples show an intense endotherm with a maximum at 825–845 °C, which is related to the dissociation of the $CaCO_3$ of dolomite and calcite. This peak is preceded by a moderate endothermic one occurring between 650 and 750 °C due to the dissociation of the $MgCO_3$ of dolomite. These two endotherms are associated with a loss in weight of 19.15 and 26.66% for DP and DI, respectively. The loss in weight detected for the dissociation of dolomite in HP and HI is 5.93 and 10.62%, respectively. This loss is accompanying the decomposition of its dolomite content with a moderate endothermic peak existing between 650 and 750 °C as shown in Fig. 2. The presence of higher magnesite content in HP and HI samples as compared with DP and DI is confirmed by the more intense endothermic peak at 650–670 °C. Also the loss in weight associating magnesite dissociation at this temperature decreases in the order HP > HI > DP > DI. In contrast, the loss detected for calcareous minerals, i.e. dolomite and calcite existing between 650 and 670 °C increases in the same order as shown in Fig. 3. This indicates that the amount of calcareous minerals increases in this order at the

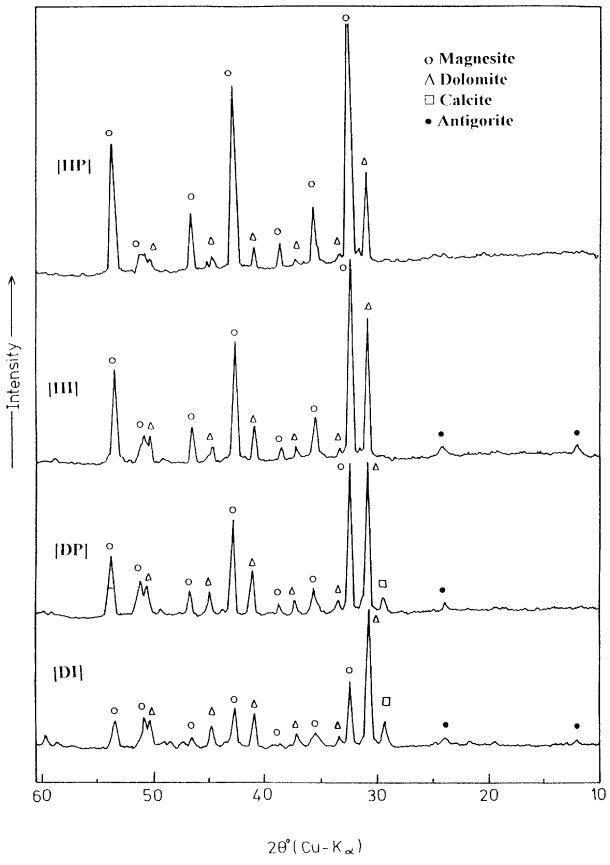


Fig. 1. XRD patterns of the raw magnesite samples.

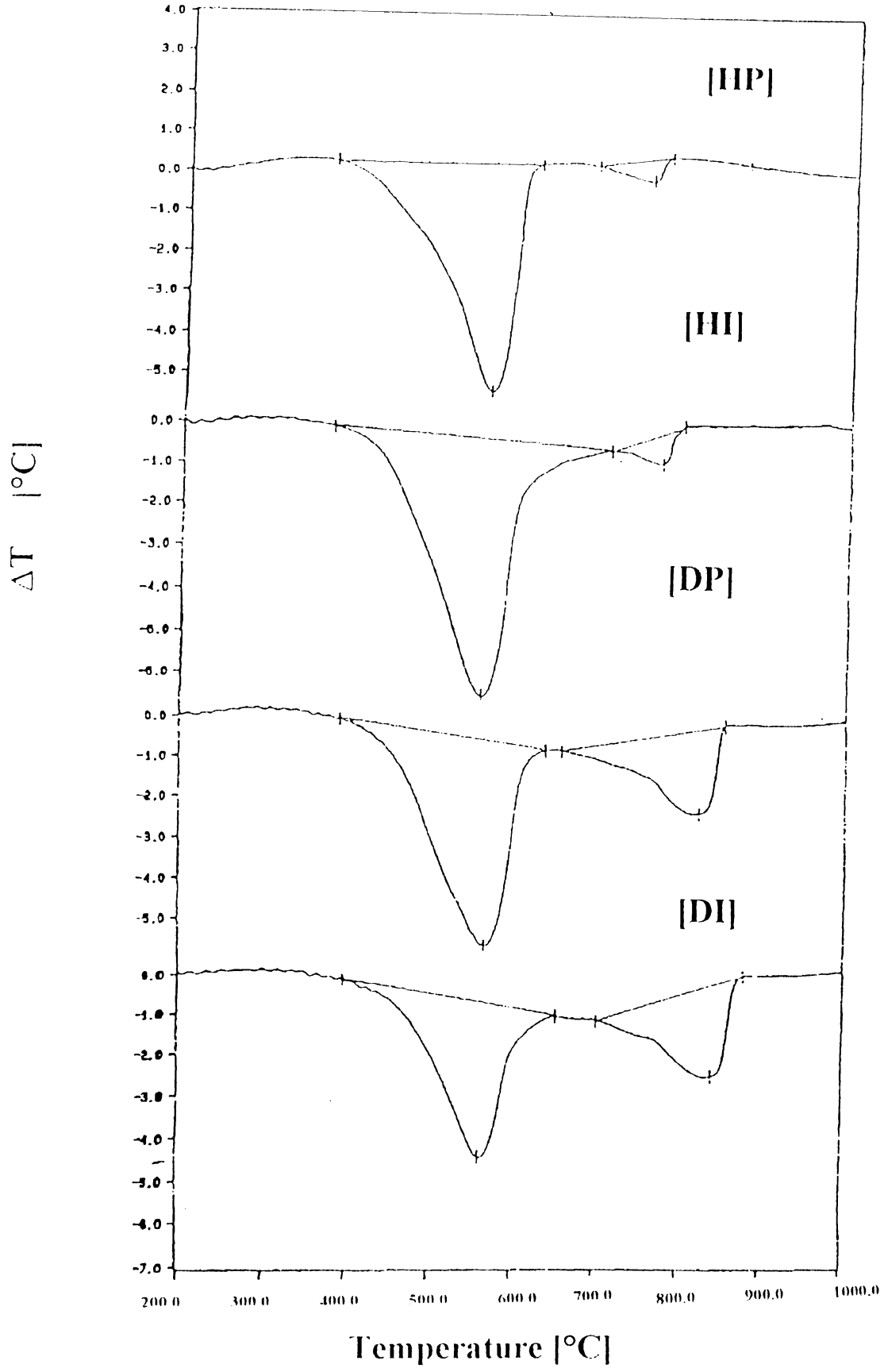
[HP]
[HI]
[DP]
[DI]
ΔT [°C]
Temperature [°C]
200.0
300.0
400.0
500.0
600.0
700.0
800.0
900.0
1000.0

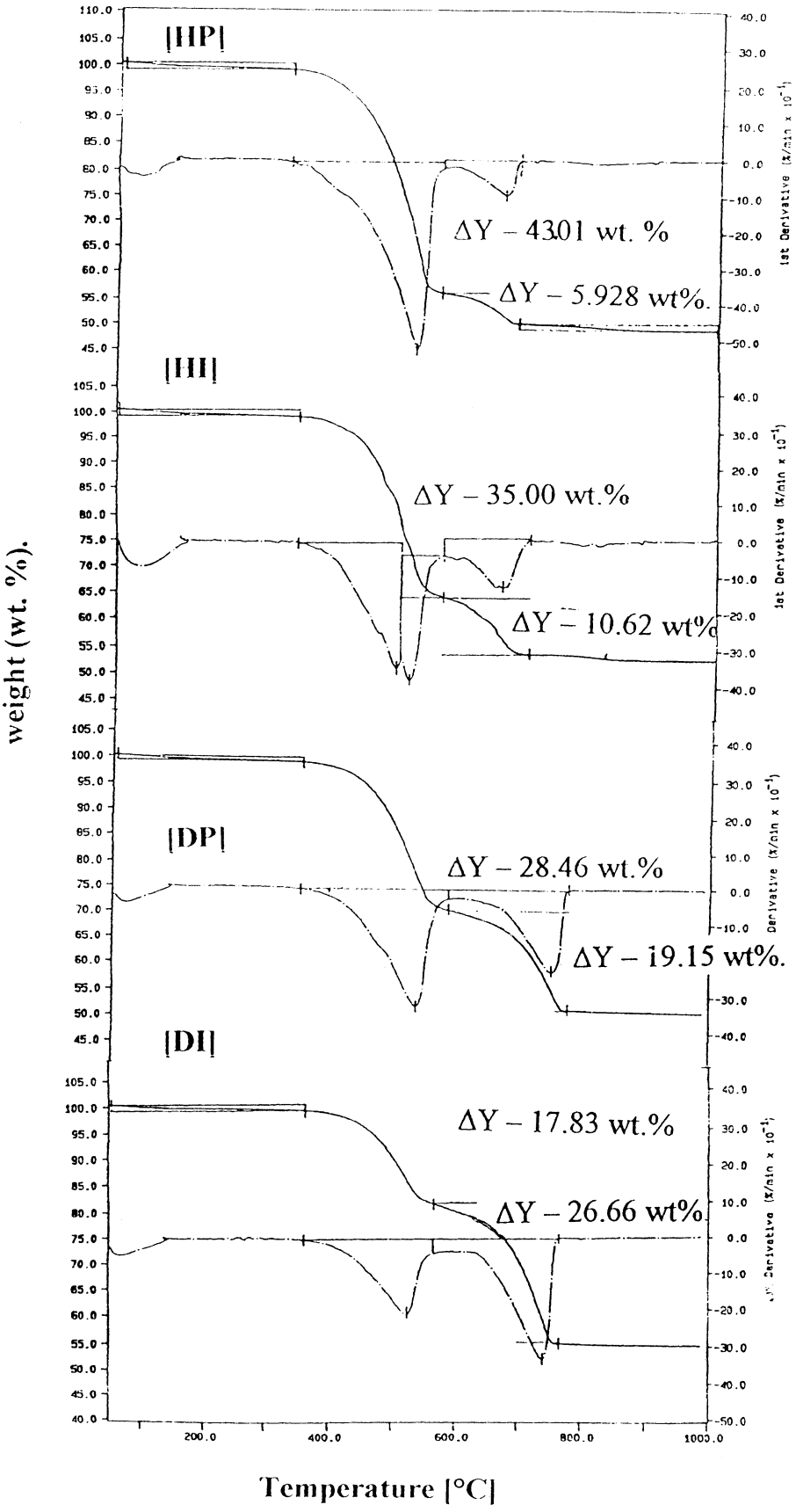


Fig. 3. TG and DTG curves of the raw magnesite samples.

expense of magnesite mineral, i.e. calcite and/or dolomite [9,10].

Table 1 summarizes the chemical analysis data of the raw magnesite samples. These results confirm the increase of calcareous minerals; namely, calcite and/or dolomite at the expense of magnesite in the order HP < HI < DP < DI. This is indicated from the gradual decrease of the MgO/CaO ratio and loss on ignition in this direction. Also, the presence of a higher amount of serpentine minerals in HI and DI as compared with HP and DP samples is seen from their relatively higher $SiO_2$ and $Fe_2O_3$ contents; 2.6–2.9 and 1.2–1.6%, respectively. In addition the results of Table 1 also indicate relatively higher $Al_2O_3$ content in hill magnesite samples (1.0 and 1.9% in HP and HI) in comparison with those of dome and vein samples (0.2–0.4% in DP and DI).

It is concluded that all samples representing the magnesite ores of the Sul Hamed area belong to the calcareous magnesite type with variable calcite and/or dolomite minerals as well as MgO/CaO ratio. This ratio exists at a relatively higher level in samples collected from hills, which include the main magnesite reserve (about 460,000 ton) as compared with those of dome and vein samples. Both magnesite occurrences are classified into pure and impure categories according to their contamination with antigorite. All of these samples need to be assessed in the preparation of shaped and unshaped MgO–CaO refractories.

Densification parameters of HP, HI, DP and DI samples in terms of bulk density, apparent porosity and linear shrinkage have been studied as a function of firing temperature up to 1550 °C. The solid-phase composition of the fired samples have been calculated according to White [11] and qualitatively determined by XRD. These results are interpreted in relation to thermal equilibrium data calculated for the fired samples using the relevant phase equilibrium diagrams [12,13].

Fig. 4 illustrates the densification parameters of the magnesite samples fired between 1300 and 1550 °C as a function of firing temperature. It is evident that the impure magnesite sample HI, with the highest content of impurity oxides, i.e. $SiO_2$, $Al_2O_3$ and $Fe_2O_3$ (11.8%), as illustrated in Table 1, exhibits the highest degree of densification at all firing temperatures. The rate of densification is appreciably enhanced at ⩾1400 °C giving maxima of bulk density (2.27–2.29 g/cm$^3$) and linear shrinkage (28.0–29.0%) with a minimum apparent porosity lower than 1.0%. This is mainly attributed to its highest content of impurity oxides that lead to the formation of equivalent amounts of calcium silicate as well as calcium and magnesium alumino- ferrite phases. These phases coexist beside the major periclase (MgO) phase on firing HI up to the sub-solidus temperatures of such phase assemblage (less than 1300 °C). Up to this temperature, the highest content of the low-melting $C_4AF$ (8.1%) is formed, beside 5.9% spinel solid solution (MA–MF), 15.9% $C_2S$ and 70.1% free periclase as calculated in Table 2. The formation of these phases is qualitatively confirmed by XRD as shown in Fig. 5. Calcium silicate phases ($C_3S$ and $C_2S$) could not be

Table 1
Chemical composition of the raw magnesite samples

| Oxides (wt.%) | HP | HI | DP | DI |
|---|---|---|---|---|
| $SiO_2$ | 0.54 | 2.85 | 0.39 | 2.60 |
| $Al_2O_3$ | 1.02 | 1.94 | 0.40 | 0.24 |
| $Fe_2O_3$ | 0.48 | 1.28 | 0.60 | 1.60 |
| CaO | 6.31 | 8.56 | 14.30 | 19.64 |
| MgO | 40.35 | 36.92 | 35.30 | 29.05 |
| L.O.I | 50.98 | 48.14 | 48.84 | 46.57 |
| Total | 99.68 | 99.69 | 99.83 | 99.70 |

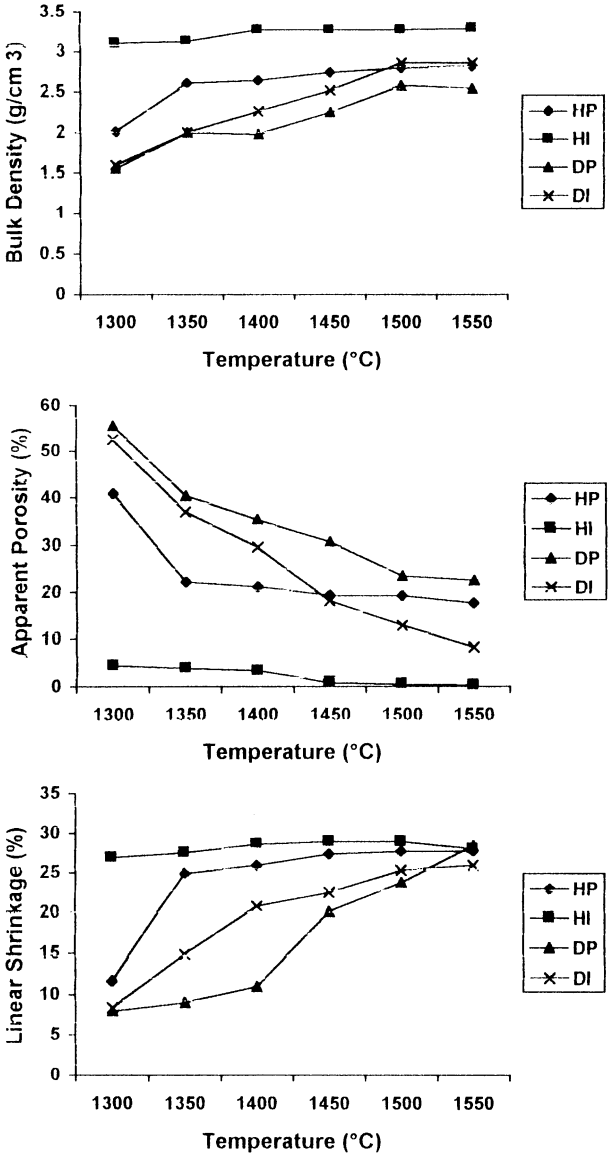


Fig. 4. Densification parameters of HP, HI, DP and DI samples as a function of firing temperature.

easily detected due to their small amounts and/or overlapping of their XRD lines with other calcium compounds.

At the quaternary eutectic point of the above phase assemblage ($T_E = 1295$ °C), all of $C_4AF$ enters the eutectic liquid phase, beside some of MF, MA, $C_2S$ and MgO phases in descending order. The content of liquid phase formed at 1300 °C in HI as calculated in Table 3 amounts to 17.2%. This liquid phase coexists with 13.5% $C_2S$ and 69.3% MgO. At 1550 °C, a higher amount of liquid phase is developed at the expense of $C_2S$ and MgO. The residual amounts of these phases (9.2 and 68.3%, respectively) coexist with 22.4% of liquid phase at 1550 °C. The development of such high amount of basic liquid phase, i.e. lime-rich liquid phase up to 1550 °C is the main reason responsible for maximizing bulk density at $\geqslant$1400 °C as well as linear shrinkage of HI and minimizing apparent porosity as shown in Fig. 4. Such liquid phase has low viscosity and is capable of flowing within the interstitial spaces of the residual solid phases leading to the closure of most of the open pores. On cooling, the dissolved phases, i.e. MgO, $C_2S$, MA–MF and $C_4AF$ are gradually recrystallized into fine particulates in the matrix of coarser particles of the residual periclase particles.

The microstructure of HI sample fired up to 1550 °C as shown in Fig. 6 confirms the above thermal equilibrium data. Rounded periclase particles (dark) with variable sizes are shown embedded in a calcium–alumino-ferrite (bright) and -silicate phases (grey). The point analysis of the largest periclase particle (No. 1 in Table 4) indicates the coexistence of some lime (CaO) and iron ($Fe_2O_3$) as solid solutions in the periclase and the calcium–silicate phase. This means that HI becomes stable against reaction with water vapour after firing up to 1550 °C. Hence, it is suitable for the production of stabilized MgO–dolomite refractories without any additions [2,4].

Similarly, the DI sample is suitable for processing semi-stable MgO–dolomite refractories, but after adding more iron oxides to accelerate its densification up to 1550 °C. This is mainly due to its relatively lower MgO/CaO ratio as well as total impurity oxides as compared with HI sample (see Table 1). On firing up to $<$1300 °C, $C_3S$ (18.6%) and $C_4AF$–$C_2F$ solid solution (6.0%) are formed and coexist with free lime (20.7%) and periclase (54.7%) phases as calculated in Table 3. At 1300 and 1550 °C, 9.6 and 15.0% liquid phase is formed at the cost of $C_4AF$–$C_2F$, $C_3S$, CaO and MgO in decreasing order as calculated in Table 3. On cooling, the dissolved phases are recrystallized down to 1300 °C in inverse order. The XRD pattern of DI fired up to 1550 °C confirms such solid phase composition as shown in Fig. 5. Also, the arrangement of these phases as revealed by SEM in Fig. 6 and its point analysis in Table 4 confirm the presence of dark periclase solid solution particles surrounding smaller particles of lime (very bright), calcium silicate (grey) and alumino-ferrite

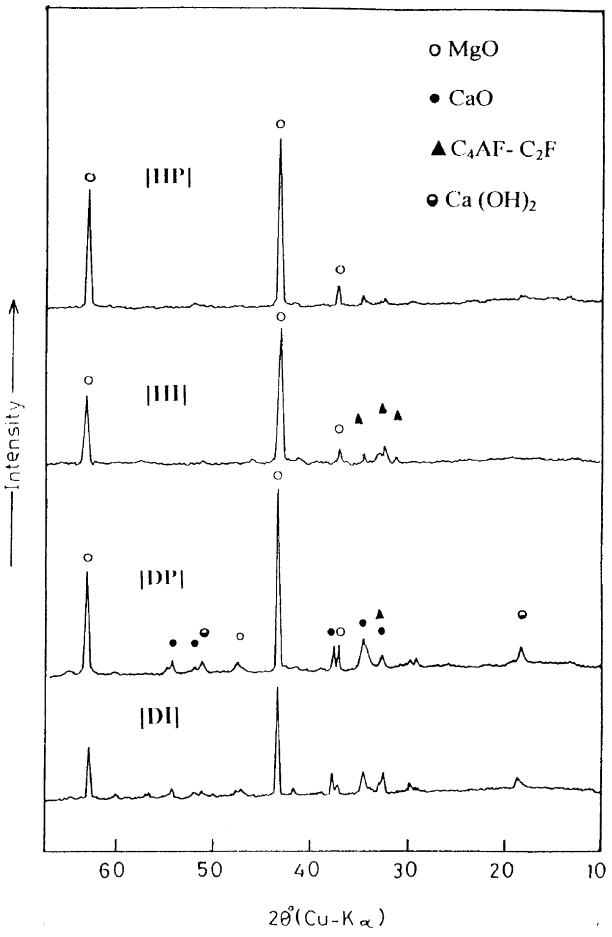


Fig. 5. XRD patterns of the raw magnesite samples after firing for 2 h at 1500 °C.

Table 2
Calculated chemical and phase composition of the raw magnesite samples after firing up to 1550 °C

| Sample symbol | Chemical composition (wt.%) | | | | | C/S molar ratio | Phase composition (wt.%) | | | | | | | | |
|---|---|---|---|---|---|---|---|---|---|---|---|---|---|---|---|
| | $SiO_2$ | $Al_2O_3$ | $Fe_2O_3$ | CaO | MgO | | $C_3S$ | $C_2S$ | $C_4AF$ | $C_2F$ | $C_3A$ | MA | MF | CaO | MgO |
| HP | 1.11 | 2.09 | 0.99 | 12.96 | 82.85 | 12.51 | 4.22 | – | 2.54 | – | 3.86 | – | – | 6.53 | 82.9 |
| HI | 5.53 | 3.76 | 2.48 | 16.61 | 71.62 | 7.03 | – | 15.9 | 8.1 | – | – | 4.2 | 1.7 | – | 70.2 |
| DP | 0.76 | 0.79 | 1.18 | 28.05 | 69.23 | 39.44 | 2.89 | – | 3.60 | – | 0.11 | – | – | 24.19 | 69.2 |
| DI | 4.89 | 0.45 | 3.01 | 36.97 | 54.68 | 8.10 | 18.58 | – | 2.14 | 3.91 | – | – | – | 20.7 | 54.7 |

solid solution (bright) phases. Also, some inter and intra pore spaces (dark) are detected.

According to the above results, lesser liquid phase content is developed in DI up to 1550 °C as compared with HI. Also, DI contains relatively higher free lime (20.7%) and lower periclase (54.7%) as compared with those of HI (0.0 and 70.1%, respectively). Hence, DI shows appreciably lower rate of densification on firing between 1300 and 1550 °C as shown in Fig. 4. The bulk density and linear shrinkage are gradually increased up to 2.86 g/cm$^3$ and 25.9%, respectively with parallel decrease of apparent porosity down to 8.3%.

In order to improve the rate of densification of DI, a limited amount of a fluxing agent, e.g. $Fe_2O_3$, should be added to such magnesite sample. This leads to the formation of more calcium alumino-ferrite phases, which stimulates the role of liquid phase in its densification up to 1550 °C. Hence, it is recommended to apply such magnesite sample for the production of semi-stable MgO-dolomite refractories after adding a limited amount of iron oxides [2,4,14].

Concerning the densification of the pure HP and DP samples, both show slower rate of densification than for the impure HI and DI samples; especially at 1500–1550 °C.

Table 3
Thermal equilibrium data calculated for magnesia–dolomite refractions in the solid state and at 1300 and 1550 °C

| Batch symbol | Wt.% of phase composition at (°C) | | | | | | | | | | | | | | | | | | |
|---|---|---|---|---|---|---|---|---|---|---|---|---|---|---|---|---|---|---|---|
| | <1300 | | | | | | | | | 1300 | | | | | 1550 | | | | |
| | MgO | CaO | $C_3S$ | $C_2S$ | $C_4AF$ | $C_2F$ | $C_3A$ | MF | MA | Liquid phase | MgO | CaO | $C_3S$ | $C_2S$ | Liquid phase | MgO | CaO | $C_3S$ | $C_2S$ |
| HP | 82.9 | 6.5 | 4.2 | – | 2.5 | – | 3.9 | – | – | 8.4 | 82.5 | 7.0 | 2.1 | – | 13.4 | 81.2 | 5.4 | – | – |
| HI | 70. | – | – | 15.9 | 8.1 | – | – | 1.7 | 4.2 | 17.2 | 69.3 | – | – | 13.5 | 22.4 | 68.3 | – | – | 9.2 |
| DP | 69.2 | 24.2 | 2.9 | – | 3.6 | – | 0.1 | – | – | 5.4 | 69.0 | 24.2 | 1.5 | – | 7.8 | 68.7 | 23.5 | – | – |
| DI | 54.7 | 20.7 | 18.4 | – | 2.1 | 3.9 | – | – | – | 9.6 | 54.2 | 20.2 | 16.1 | – | 15.0 | 53.6 | 20.8 | 10.7 | – |

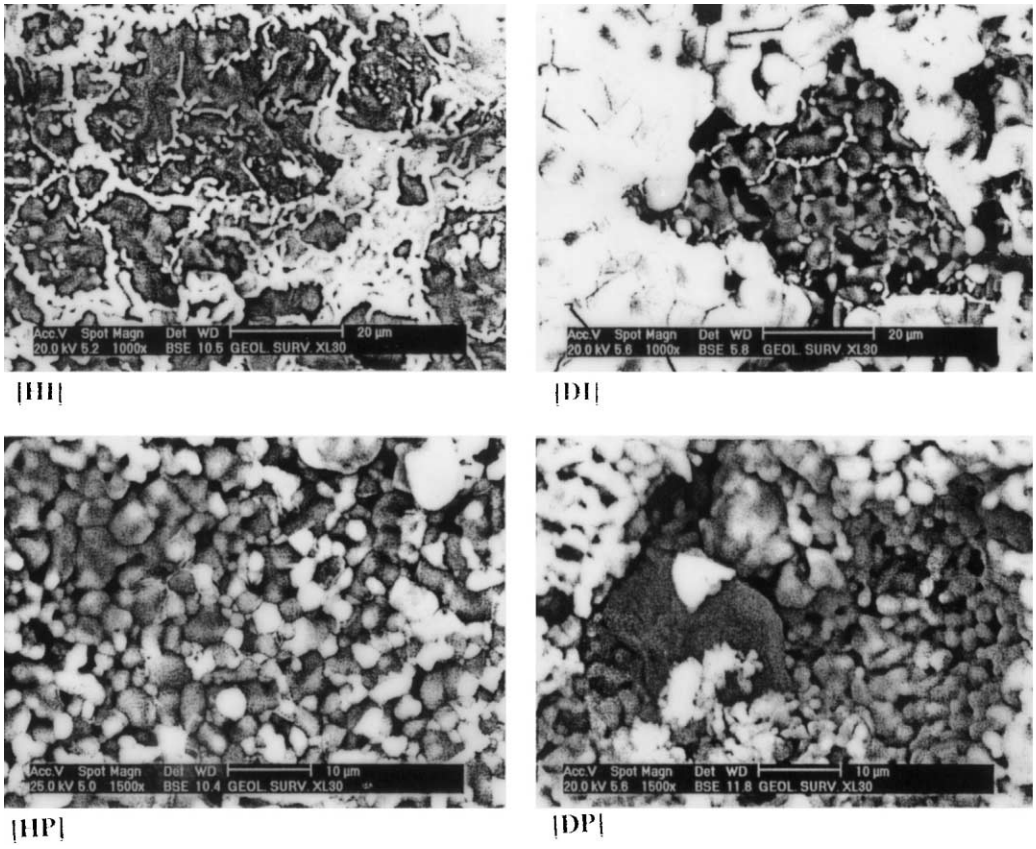


Fig. 6. SEM photomicrographs of HI, DI, HP and DI samples fired up to 1550 °C.

Table 4
Point analyses data of HI, DI, HP and DP raw magnesite samples fired up to 1550 °C

| Oxide% | HI | | | | DI | | | HP | | | DP | | |
|---|---|---|---|---|---|---|---|---|---|---|---|---|---|
| | 1 | 2 | 3 | 4 | 1 | 2 | 3 | 1 | 2 | 3 | 1 | 2 | 3 |
| $SiO_2$ | 25.76 | 6.21 | 23.95 | 1.64 | 33.02 | – | 10.17 | – | 19.33 | 27.53 | 1.06 | – | 16.51 |
| $Al_2O_3$ | – | 1.85 | – | 0.71 | – | – | 1.17 | – | – | 2.91 | 3.66 | 10.99 | – |
| $Fe_2O_3$ | 2.40 | 5.29 | 3.45 | 1.30 | 2.61 | – | 4.97 | – | 1.08 | 3.40 | 3.03 | 16.10 | – |
| MgO | – | 68.67 | – | 93.39 | – | 100.00 | 12.73 | 98.19 | 43.25 | 1.46 | 74.52 | 21.43 | 42.05 |
| CaO | 70.72 | 17.98 | 72.60 | 2.97 | 64.37 | – | 70.96 | 1.81 | 33.88 | 62.03 | 17.72 | 51.48 | 41.44 |
| $P_2O_5$ | – | – | – | – | – | – | – | – | 2.46 | 2.66 | – | – | – |
| $SO_3$ | 1.12 | – | – | – | – | – | – | – | – | – | – | – | – |

However, HP exhibits relatively higher densification rate than DP on firing between 1300 and 1450 °C. This is mainly attributed to the relatively lower content of total impurity oxides in HP and DP (4.2 and 2.7%, respectively) as compared with HI and DI (11.8 and 8.4%, respectively). Also, the significantly higher MgO/CaO ratio of HP than DP has contributed in the relative increase of its densification at 1300–1450 °C as compared with the latter one.

Due to the high $CaO/SiO_2$ molar ratio of HP and DP (12.5–39.4), both have the same phase assemblage as calculated in Table 3. Limited amounts of $C_3S$, $C_4AF$, $C_3A$ are formed in both samples, beside the major phases periclase and lime with higher periclase/lime ratio in HP as compared with DP. Such solid-phase composition is expected in these samples, after firing up to 1550 °C. The XRD patterns of HP and DP samples fired up to 1550 °C (Fig. 5) show the same phases with higher free lime content in DP due to presence of CaO (14.3%) in the original sample. In addition, some of the free lime is hydrated into $Ca(OH)_2$ during the preparation of these samples for XRD analysis.

According to the thermal equilibrium data calculated for HP and DP samples from the modular system of the $MgO–CaO–C_3S–C_4AF$,a liquid phase is expected to be formed on firing up to $T_E = 1295$ and 1550 °C as illustrated in Table 3. Generally, HP gives relatively higher liquid phase content (8.4 and 13.4%) as compared with DP (5.4 and 7.8%) at 1300 and 1550 °C, respectively. The liquid phase is mainly formed and developed at the expense of calcium alumino-ferrite phases and also by limited and gradual dissolution of free periclase and lime phases. This accounts for the relatively higher densification rate of HP in comparison with DP on firing up to 1550 °C. Hence, HP gives relatively higher bulk density (2.82 $g/cm_3$) and linear shrinkage (27.7%) with lower apparent porosity (17.6%) than the corresponding of DP (2.54 $g/cm^3$, 24.1% and 22.6%, respectively). The coexistence of higher free lime content in DP together with periclase up to 1550 °C leads also to further inhibition of the densification of such MgO–CaO refractory grains [14].

The study of microstructure of HP and DP samples fired up to 1550 °C as shown in Fig. 6 confirms their densification and thermal equilibrium data. Both samples show grown periclase particles containing CaO and $Fe_2O_3$ in solid solution (dark) interlocked with smaller particles of lime (light grey) and both are embedded in a matrix composed of finer crystals of $C_3S$ (grey) and calcium alumino-ferrite phases (bright). The coexistence of these phases in the solid state is confirmed by their point analyses as illustrated in Table 4. These data also confirm the relatively higher periclase/lime ratio of HP than DP. In addition, both samples enclose open and closed pores (dark) indicating their low degree of densification after firing up to 1550 °C.

Accordingly, the pure HP and DP dolomitic magnesite samples of Sul Hamed area are recommended for the production of the unshaped MgO–CaO refractories. For manufacturing such refractory products minimum $SiO_2$ (less than 3.0%) and high $Fe_2O_3$ and $Al_2O_3$ (7–9%) with a sufficient amount of lime (10–15%) and periclase (70–80%) are required [3,4]. Therefore, HP with adequate contents of lime (13.0%) and MgO (82.9%) is recommended for the production of dense MgO–CaO unshaped concrete after firing up to 1550 °C with addition of a sufficient amount of iron oxides as sintering aid. On the other, hand, DP can be similarly applied after rising MgO/CaO ratio and $Fe_2O_3$ contents with the addition of sufficient amounts of used magnesite bricks as well as waste iron oxide material [15].

## 4. Conclusions

The major amount of dolomitic magnesite ore exists as hills with relatively higher MgO/CaO ratio than the minor amounts occurring as domes and veins due to the higher content of calcite and/or dolomite in the latter type.

Both ore deposits are classified into pure and impure categories according to the degree of their contamination with the coloured serpentine and iron oxide minerals.

Pure dolomitic magnesite ore is recommended for the production of unshaped MgO–CaO refractories with the addition of MgO-rich and/or $Fe_2O_3$-rich materials, before firing up to 1450–1550 °C.

Impure ore can be utilized in the production of stabilized and semi-stabilized MgO–dolomite refractories with and without addition of proper amounts of iron-rich material before firing.

## References


[1] K. Shaw, Refractories and their Uses, Applied Science Publishers, London, 1972.

[2] J.H. Chesters, Refractories: Production and Properties, Iron and Steel Institute, London, 1973.

[3] S.C. Carniglia, G.L. Barna, Handbook of Industrial Refractories Technology, Noyes Publications, Park Ridge, NJ, USA, 1992.

[4] G. Routschka (Ed.), Pocket Manual, Vulkan Verlag, Essen, Germany, 1997

[5] A. Mazhar, Z. El-Alfi, B.B. Nasr, M.F. Sadek, M.A. Dallal, A. Manzour, A.A. El-Sarti, M. Eskender, A.A. Sedeik, A. Rasmy, Occurrence of Magnesite Ores in Eastern Desert, Egypt, Geol. Surv. Int. Report, N 45/98 in Arabic, 1998, 90 p.

[6] A. Hussein, Mineral deposits, in: R. Said (Ed.), The Geology of Egypt, Balkema, Rotterdam book field, 1990, pp. 511–566.

[7] M.M. Hassaan, Y.A. Elsheshtawi, T.M. Ramadan, A.M. Elgharib, Geological and Geochemical Studies on Serpentinites and Magnesite Deposits, Sul Hamed Area Eastern Desert Egypt with Emphasis on their Economic Aspects, Mineral deposits, Balkema, Rotterdam, 1997, pp. 725–728.

[8] M.S. Elmaghraby, Mineralogical and geochemical studies of magnesite deposits, South Eastern Desert and its assessment for production of refractories, PhD thesis, Geology department, Faculty of Science, Ain Shams University, Cairo, Egypt, 2001.

[9] R.C. Mackenzie, Differential Thermal Analysis, Vol. 1, Academic Press, London and New York, 1970.

[10] N.T. Dumitru, Thermal Analysis of Minerals, ABACU Press, United Kingdom, 1976.

[11] J. White, Recent developments in research on basic refractories, Refractories J. 46 (1) (1970) 6–18.

[12] M.A. Serry, A. Barbulescu, Thermal equilibrium of MgO–dolomite refractories within the system CaO–MgO–$C_4AF$-$C_2S$, Trans. J. Br. Ceram. Soc. 80 (6) (1981) 196–201.

[13] S. Solacolu, The system MgO–$C_3S$–$C_2S$–$C_4AF$, Ber. Deut. Keram. Ges. 34 (1957) 141–147.

[14] M.A. Serry, M.S. Attia, Thermal equilibrium and properties of some MgO–dolomite refractories, Trans. J. Br. Ceram. Soc. 84 (4) (1985) 142–145.

[15] M.A. Serry, H.S. Abd-Elwahab, A.A. Abd Allah, Properties and performance of refractory MgO–CaO fettling concretes as related to their composition and microstructure, Silicate Industriels 64 (1–2) (1999) 87–93.